JOURNAL OF AIRCRAFT
Vol. 45, No. 4, July–August 2008

Tip-Disturbance Effects on Asymmetric Vortex Breakdown Around a Chined Forebody

Bao-Feng Ma* and Xue-Ying Deng†
Beijing University of Aeronautics and Astronautics, 100083 Beijing, People's Republic of China

DOI: 10.2514/1.31352

An experimental study about the tip-disturbance effects on the asymmetric vortex breakdown of a chined forebody was conducted using a wing–body model. The vortices of the chined forebody could produce an asymmetric breakdown at high angles of attack when adding an artificial disturbance onto the nose tip. The forebody vortex with asymmetric breakdown would further interact with the vortices of the strake and wing, consequently inducing significant differential loads on two sides of the wing. When the tip disturbance was located on the leeward side and approached the nose tip, the disturbance had a more prominent effect on the asymmetric breakdown. Moreover, the asymmetry level of the vortex breakdown would increase with increasing geometric sizes of the tip disturbance. However, when a splitter plate was placed in the leeward symmetry plane of the model, the asymmetry of the vortex breakdown would disappear, even adding a tip disturbance.

Nomenclature

C_p	=	pressure coefficients, $Cp = (P - P_\infty)/(1/2\rho U^2)$
p_∞	=	freestream static pressure
Re	=	Reynolds number based on root-chord length of the wing L, UL/ν
U	=	freestream velocity
α	=	angle of attack
ξ_x	=	local nondimensional coordinates based on characteristic scale that is the sectional circumference at sections S1–S8 and the curve length of the upper surface of the section at sections S9–S19

Subscript

x	=	measurement-sections index, S1–S19

I. Introduction

MODERN aircraft increasingly used a chined forebody for lower observability, a larger lift force, and better high-speed performances. The aerodynamic characteristics of a chined forebody were very different from the ones of a traditional smoothed-side forebody at high angles of attack. The smoothed-side forebody could produce an asymmetric vortical flow at high angles of attack, which would induce a quite large side force and yawing moment. The previous studies have revealed that small geometric imperfection on the nose tip would be responsible for the asymmetric vortex due to the intrinsic instability of the flowfield itself [1,2]. Many tip-control techniques to the asymmetric vortex have been proposed and implemented based on the asymmetric vortex sensitivity to the nose tip [3,4]. However, for a chined forebody, the vortical flow over it was relatively stable and almost no asymmetric vortex could be produced before vortex breakdown occurred [5–7], because its separation line was fixed at a sharp side edge. Therefore, the flow feature around a chined forebody more resembles the one around a high-sweep delta-wing with a sharp leading edge [8,9], rather than the one around a smoothed-side forebody. Many approaches also have been used to control the vortex over a chined forebody, but most of these approaches required adding large external energy into the flowfield [10–13], and the methods based on the tip micro-perturbation became ineffective, because the flowfield itself lacked the instability like that of the vortical flow over a smoothed-side forebody.

Although no vortex asymmetry existed over a chined forebody, vortex breakdown over it was more prone to occur at high angles of attack than that over a smoothed-side forebody. Kegelman and Roos [6] and Mange and Roos [7] found that vortex breakdown over an isolated chined forebody was so asymmetric to induce symmetric loads on the forebody. They suggested that the asymmetric vortex breakdown came from imperfection of the nose tip, but no further work has been conducted to verify this idea. Lowson and Riley [14] also found that even over delta wings, vortex breakdown was also so sensitive to the apex that the locations of vortex breakdown could be accelerated or delayed by using a movable apex flap. The preceding research implied that the nose tip had an important effect on vortex breakdown, and little imperfection of the tip might cause a very large variation on vortex-breakdown patterns. To study the nose-tip effect on the asymmetric vortex breakdown, a good strategy was to add an artificial disturbance to the nose tip and then study the response of vortex breakdown to it, as done in the study on vortex asymmetry over a smoothed-side forebody [15].

In addition, vortex interactions of a chined forebody with other components, such as a wing or strake, was also an important problem studied extensively. The experimental results by Erickson and Brandon [16] and Hall [17] have shown that a chined-forebody vortex could delay the wing vortex breakdown through a beneficial vortex interaction. Therefore, when asymmetric breakdown occurred for a chined-forebody vortex, how it would affect the wing vortex is also a problem that should be investigated further.

The objective of the present investigation was to investigate the response of the asymmetric breakdown of the chined-forebody vortex to a tip disturbance. Specifically, the following three questions would be answered: First, could an artificial tip disturbance influence the asymmetric breakdown of the chined-forebody vortices? And, if so, how would it influence it? Second, how would the chined-forebody vortex with asymmetric breakdown influence the wing vortex and the model loads through vortex interactions? Third, would the vortex-breakdown asymmetry vary with the position and magnitude of the tip-disturbance?

II. Experimental Setup

The experiments were conducted in the D4 low-speed wind tunnel of the Institute of Fluid Mechanics of Beijing University of

Received 1 April 2007; revision received 3 April 2008; accepted for publication 4 April 2008. Copyright © 2008 by Bao-Feng Ma and Xue-Ying Deng. Published by the American Institute of Aeronautics and Astronautics, Inc., with permission. Copies of this paper may be made for personal or internal use, on condition that the copier pay the $10.00 per-copy fee to the Copyright Clearance Center, Inc., 222 Rosewood Drive, Danvers, MA 01923; include the code 0021-8669/08 $10.00 in correspondence with the CCC.

*Postdoctoral Associate, Ministry-of-Education Key Laboratory of Fluid Mechanics; bf-ma@buaa.edu.cn.

†Professor, Ministry-of-Education Key Laboratory of Fluid Mechanics; dengxueying@vip.sina.com. Senior Member AIAA.

Aeronautics and Astronautics. The wind tunnel is a low-speed, low-noise, closed-return tunnel that can be run with either an open or closed test section. The test sections are 1.5 m wide, 1.5 m high, and 2.5 m long, with a turbulence level of less than 0.1%. The open test section was used in the present experiments.

The experimental model is shown in Fig. 1. The model is a strake–wing–body configuration with a chined forebody. The chined forebody has a sharp side edge and the included angle of the chine was 104 deg. The strake and the wing have a small radius, blunt leading edge and the sweep angles are 72 and 42 deg, respectively. The strake and wing are coplanar and high mounted. Moreover, the strake is removable, and can be removed if required. All components of the model were made from aluminum. The model was sting mounted. A disturbance was placed on the nose tip of the chined forebody. Several types of disturbance were used and will be described in detail in the next section.

The model was equipped with many pressure taps arranged in 19 sections (S1–S19). The pressure taps were distributed across the leeward and windward surfaces of the model in sections S1–S8, and only the leeward surface in sections S9–S19. The internal pneumatic tubing was stainless steel with a 0.8 mm i.d., and the tubing of stainless steel was connected with the PSI 9816 intelligent pressure scanivalve through soft rubber tubes. A total of 32 PSI 9816 modules (512 channels) with a pressure range of less than 1 psi (0.7 kPa) were equipped in the D4 wind tunnel and enough for pressure measurements of the present model.

A smoke-flow visualization experiment was carried out using steel wires of 0.1-mm-diam, and the steel wires were placed below the leading edge of the wing and the side edge of the forebody, but far away from the nose tip to avoid interference. To know whether the wires would affect the flowfield, the pressure-measurement results were compared before and after the wires were added. The results showed that the wires had almost no effect on the flowfield studied. The smoking agent was propanetriol, which could be heated to volatilize when the wires were electrified. A 5 W argon-ion laser as a sheet-light resource was used for illuminating. The recording device was a Sony DSC-V1 digital camera with a resolution of 5.25 million pixels.

All experimental data presented in this paper have proved to be repeatable, including the flow-visualization and pressure-measurement experiments. The sampling rate was set to 10 Hz and the data were averaged at each 100. The seven repeated pressure measurements based on the strake–wing–body configuration were carried out at 34.5 deg angle of attack. As can be obtained, the total standard deviation of the pressure coefficients was 0.011, the total uncertainty was ± 0.027, and the relative total uncertainty relative to the maximum pressure coefficient was 0.91%.

III. Results

A. Tip-Disturbance Effects on Asymmetric Vortex Breakdown

The investigation focused on the tip-disturbance effects on the asymmetric breakdown of the chined-forebody vortex, and so a tip disturbance of 2-cm-diam (a bead) was added onto the tip of the chined forebody, as shown in Fig. 2. The disturbance on the left side of the model was called a left disturbance and the one on the right side of the model was called a right disturbance.

Figure 3 shows the smoke-flow photographs at different measurement sections of the model at 34.5 deg angle of attack, with and without a disturbance, respectively. For the no-disturbance case, the forebody vortex (FV) was almost symmetric, as shown at sections S6 and S7 in Fig. 3. However, after adding the disturbance, the forebody vortex lost the symmetry. For the left disturbance, the position of the left-side vortex became higher than the one of the right-side vortex, and for the right disturbance, the case was contrary. The small strake of the model produced a strake vortex (SV), as shown at section S9 in Fig. 3a. The strake vortex twisted together with the forebody vortex and formed a single concentrated vortex. For simplicity, it was called a forebody-strake vortex (FSV). The forebody-strake vortex kept symmetric for the no-disturbance case, and no vortex breakdown (VB) occurred yet. However, after adding a disturbance, the vortical flow of the opposite side to the disturbance side would burst so that the flow pattern became asymmetric, as shown at section S9 in Figs. 3b and 3c.

Beyond section S9, the wing vortex (WV) was produced and the asymmetry of the forebody-vortex breakdown also caused the asymmetric breakdown of the wing vortex through vortex interactions, as shown at sections S11, S13, and S16 in Fig. 3. It should be noted that the vortex pair lost the symmetry even for the no-disturbance case at section S11, where the right vortex burst. This was because the tip imperfection arising from manufacturing tolerance could also cause the asymmetric vortex breakdown, but the level of the asymmetry was much lower. This also indicated that the vortex breakdown points for the no-disturbance case almost located near this section. For the disturbance case, the vortex breakdown on the disturbance side was delayed significantly, but that of the opposite side was accelerated. In addition, the wing vortex also exhibited asymmetric breakdown due to interaction of the forebody vortex with the asymmetric breakdown.

The asymmetric vortex breakdown and the asymmetric vortex interaction together caused an asymmetric pressure distribution on the forebody and wing, as shown in Fig. 4. The pressure distributions of the left- and right-half parts of the model were almost symmetric for the no-disturbance case. However, after adding the artificial disturbance, the suction peak on the wing of the same side with the disturbance was higher than the one on the opposite side due to the asymmetric vortex breakdown and vortex interactions. The artificial disturbance also produced asymmetric loads on the forebody due to the forebody-vortex asymmetry in the normal direction, but the asymmetry hand of the forebody loads was opposite that on the wing loads.

In the experiments, the Reynolds number for the smoke-flow visualization (0.15×10^6) was relatively low to obtain clear flow-visualization pictures, and the Reynolds number for the pressure measurements (1.35×10^6) was relatively high to obtain high measurement accuracy. Therefore, to analyze the results of the flow visualizations and pressure measurements correspondingly, it was necessary to determine the Reynolds number effects on the results. The pressure measurements at a low Reynolds number (0.15×10^6) were carried out and the results were compared with the ones at high Reynolds number, as shown in Fig. 5. It could be seen that Reynolds numbers have almost no effect on the asymmetric vortex breakdown.

The asymmetry level of vortex breakdown varies with angles of attack, as shown in Fig. 6. At 19.5 deg angle of attack, the

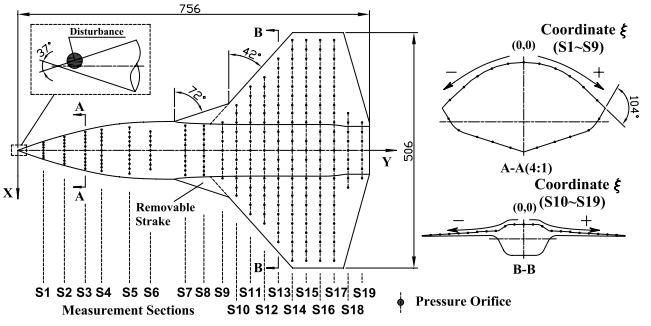

Fig. 1 Experimental model, in millimeters.

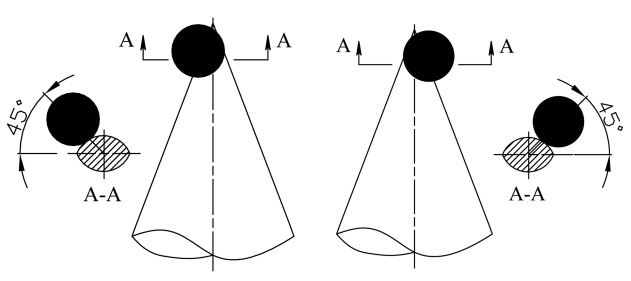

a) Left disturbance b) Right disturbance

Fig. 2 Tip disturbance.

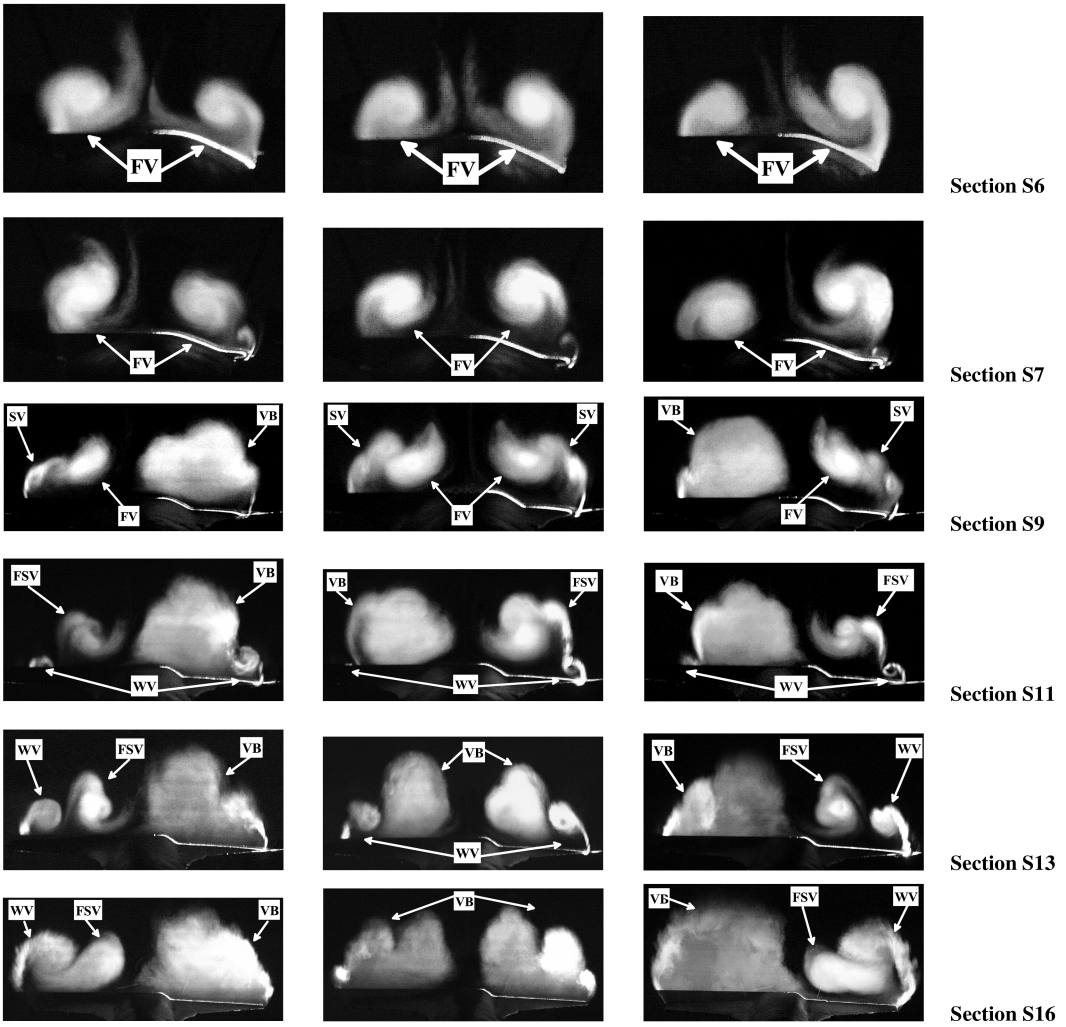

a) Left disturbance b) No disturbance c) Right disturbance

Fig. 3 Smoke-flow visualization photographs for tip-disturbance effects, $\alpha = 34.5$ deg, $Re = 0.15 \times 10^6$.

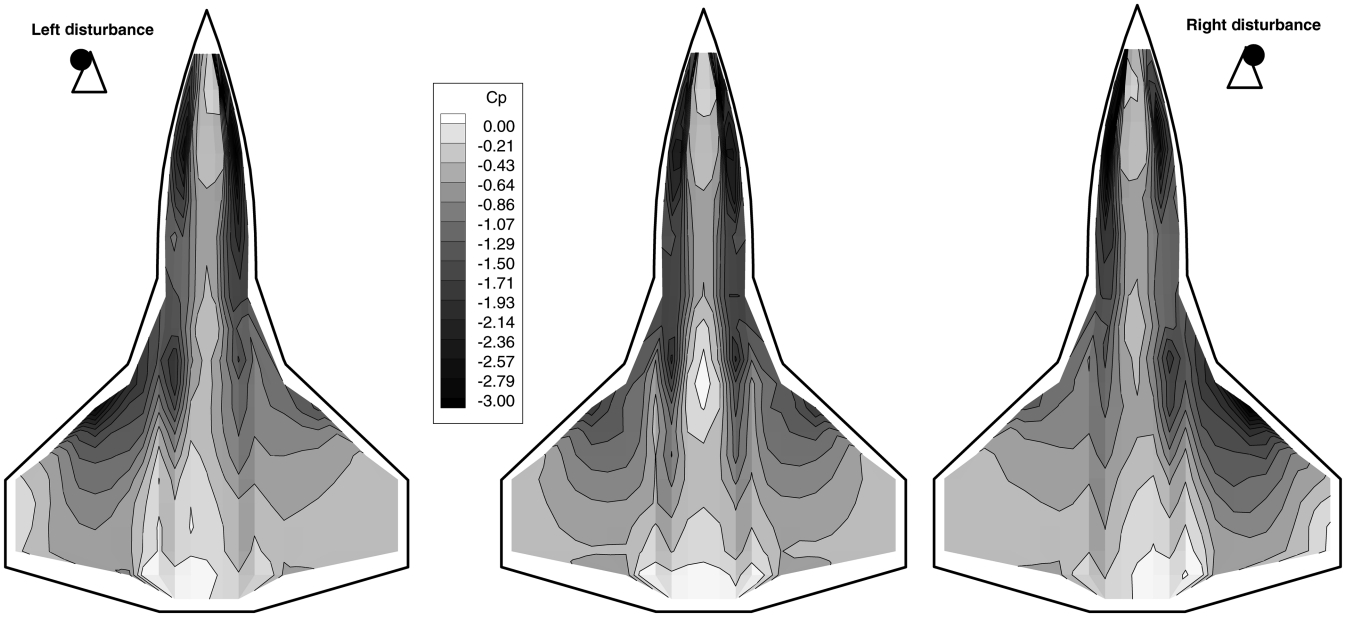

a) Left disturbance b) No disturbance c) Right disturbance

Fig. 4 Upper-surface pressure-coefficients contour of the model, $\alpha = 34.5$ deg, $Re = 1.35 \times 10^6$.

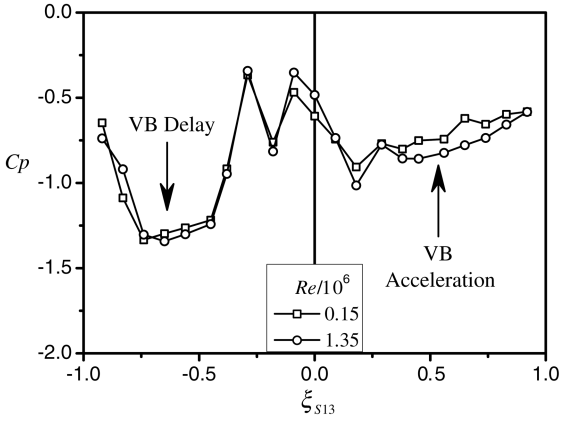

Fig. 5 Reynolds numbers effect at section S13 with left disturbance, $\alpha = 34.5$ deg.

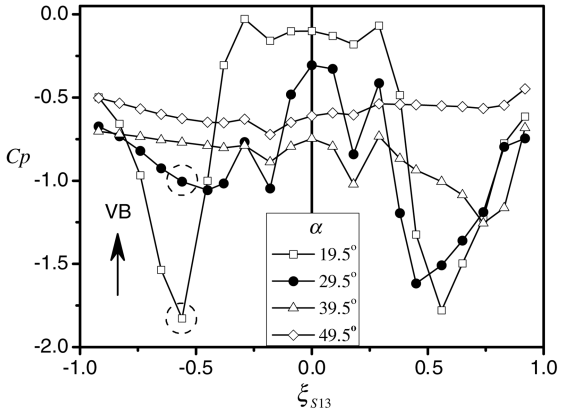

Fig. 6 Angle-of-attack effects, at section S13 with right disturbance, $Re = 1.35 \times 10^6$.

vortex-breakdown point is located far downstream after section S13. The vortical flow near section S13 was not influenced by vortex breakdown yet, and so the pressure distribution was almost symmetric. With increasing angles of attack, the vortex-breakdown points developed forward and gradually approached section S13, so that the level of the flow asymmetry was gradually enlarged, such as the case at 29.5-deg angle of attack. However, when angles of attack were high enough (more than 49.5 deg), the vortex-breakdown points passed the entire wing so that the wing was located in the wake of the vortex breakdown. As a result, the pressure distribution became symmetric again.

B. Effects of Disturbance Magnitude and Position

Three disturbances with various geometric sizes were used to determine the effects of the disturbance magnitude on the asymmetric vortex breakdown, as shown in Fig. 7a. They were called disturbance nos. 1, 2, or 3, respectively. The shape of nos. 1 and 2 is cylindrical and no. 3 is made of a folded cylinder. Figure 7b shows the asymmetry level increased with increasing geometric sizes of a disturbance. Therefore, it could be speculated that when the disturbance was smaller than a certain size, the result would be almost the same as the case for no disturbance.

Disturbance no. 2 was selected to study the position effects. The disturbance was placed on three positions, as shown in Fig. 8a. The results are shown in Fig. 8b, and it can be seen that the positions have an important effect on the asymmetric vortex breakdown. If the disturbance was located on the leeward side, the asymmetry level would become larger when the disturbance approached the nose tip, as shown in positions 1 and 2. However, the asymmetry almost disappeared when the disturbance was placed on the windward side, even if the disturbance had extremely approached the nose tip, as shown in Position 3.

C. Splitter-Plate Effects

A splitter plate was placed on the leeward side of the model aligned with the leeward symmetry plane to investigate the disturbance effect when the vortices on both sides of the model were separated, as shown in Fig. 9a. The results are shown in Fig. 9b. The presence of the splitter plate prevented vortex interaction between the two sides of the model, so that the asymmetry of vortex breakdown would disappear regardless, with or without the tip disturbance.

D. Strake-Vortex Effect

The results in Fig. 3 show that the strake vortex interacted with the forebody vortex, which made the vortex system over the model become more complicated, although the strake size was very small. To determine the effect of the strake vortex on the asymmetric breakdown of the forebody vortex, flow visualization was performed after the strake was removed. The results indicated that the tip disturbance could still cause the asymmetric breakdown of the forebody vortex. The forebody vortex with asymmetric breakdown would further cause the wing-vortex breakdown to become asymmetric even if no strake existed, as shown in Fig. 10.

IV. Discussion

A. Sensitivity of Asymmetric Vortex Breakdown to Tip Disturbance

The schematic diagram of the tip-disturbance effects on the asymmetric vortex breakdown is shown in Fig. 11 based on the preceding experimental results. The tip-disturbance effects included two processes: first, the tip disturbance resulted in asymmetric breakdown of the chined-forebody vortex; second, the chined-forebody vortices with asymmetric breakdown further interact with the vortices over the wing and strake. As a result of this interaction, the breakdown locations of the wing and strake vortices also became asymmetric. In other words, the asymmetric breakdown of the forebody vortex was attributed to the tip disturbance, but the asymmetric breakdown of the wing and strake vortices resulted from the asymmetric vortex interaction with the forebody vortex.

Regarding the first process, a tip disturbance on one side caused the vortex breakdown on that side to delay, but the vortex breakdown on the opposite side to accelerate. In fact, even with no artificial tip disturbance, the asymmetric vortex breakdown also existed, as shown at section S11 in Fig. 3b or in experiments by Kegelman and Roos [6] and Mange and Roos [7]. The nose of the present model was manufactured with a high degree of precision, so that the natural imperfection should be very small.

A remaining difficult problem concerned the mechanism of the tip-disturbance effect on the vortex breakdown. The present results were not able to answer this question, but it might be explained by analogy with the asymmetric vortex over a smoothed-side forebody. The behaviors of the asymmetric vortex breakdown much resembled the ones of the asymmetric vortex over a smoothed-side forebody, where small tip imperfection would trigger the asymmetric vortex due to the intrinsic instability of the flow itself. The present results seemed to indicate that the asymmetric vortex breakdown would also be attributed to the spatial convective instability of the forebody vortex itself. Therefore, the flowfield of the forebody vortices downstream could be regarded as a disturbance amplifier, so that a little flow change around the nose tip would be amplified to alter the flow structure downstream and produce the asymmetric vortex breakdown. It was believed that the vortex interaction between the left and right side of the forebody would play an important role during the formation of the asymmetric vortex breakdown, because the phenomenon of the asymmetric vortex breakdown would disappear if the flowfield was split using a splitter plate, as depicted in Fig. 9. However, the specific reason of the flow instability did not seem to be very clear yet. Lowson and Riley [14] proposed a candidate interpretation about this when they investigated the effect of the apex on vortex breakdown over a delta wing. They suggested that the change of the vorticity gradient in the vortex core would lead to the flow instability. Specifically, the apex shape would influence the vorticity distribution near the apex while the vorticity from the

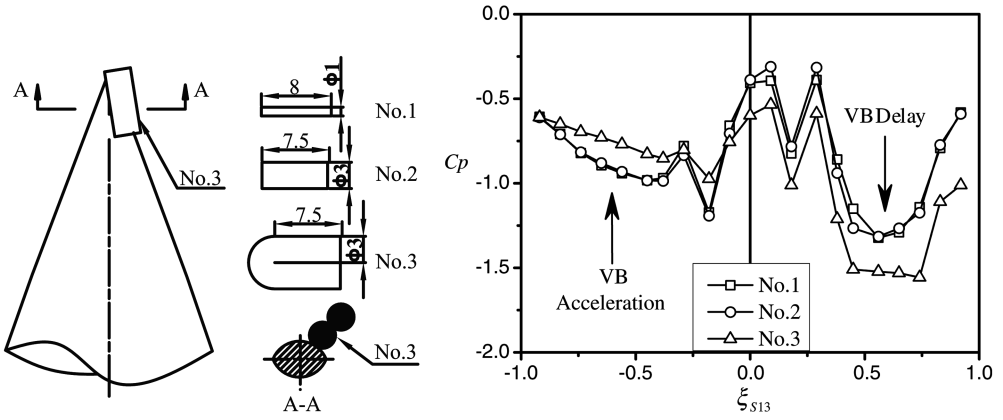

a) Various sizes of disturbance b) Effect of disturbance magnitude at section S13

Fig. 7 Effects of disturbance magnitude on asymmetric vortex breakdown, $\alpha = 34.5$ deg, $Re = 1.35 \times 10^6$.

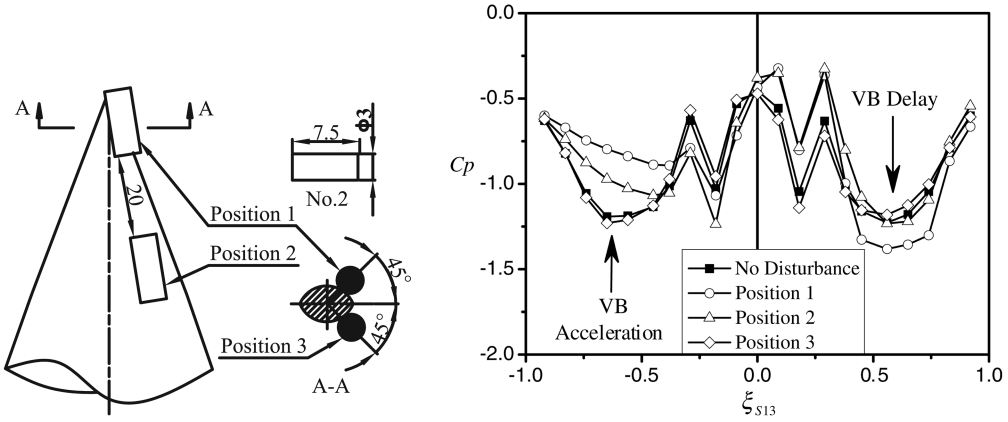

a) Various positions of disturbance b) Effect of disturbance positions at section S13

Fig. 8 Effects of disturbance positions on asymmetric vortex breakdown, $\alpha = 34.5$ deg, $Re = 1.35 \times 10^6$.

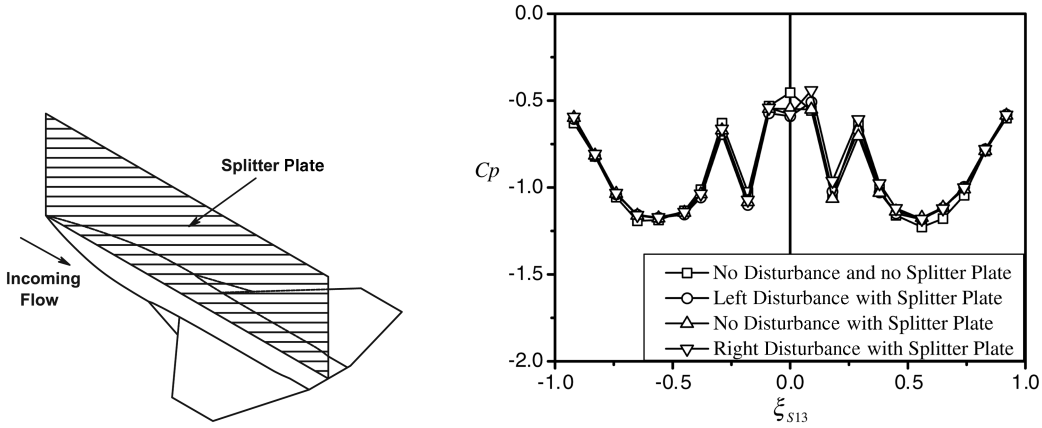

a) Splitter-plate location b) Splitter-plate effects at section S13

Fig. 9 Splitter-plate effects on asymmetric vortex breakdown, $\alpha = 34.5$ deg, $Re = 1.35 \times 10^6$.

apex formed the center of the vortex core. Therefore, the apex change would directly cause the change of the vorticity gradient in the vortex core and lead to instability. Nevertheless, this idea itself needed to be verified using further experimental or theoretical material.

The tip disturbance also made the forebody vortices slightly asymmetric in the normal direction near the nose, as shown at sections S6 and S7 in Figs. 3a and 3c. But the forebody-vortex asymmetry over the wing was not prominent, whereas the asymmetric breakdown was dominant. Therefore, the vortex asymmetry in the normal direction would have very little contribution to the loads on the wing.

The forebody vortex with asymmetric breakdown could produce an asymmetric vortex interaction and cause the asymmetric breakdown over the wing and strake vortices. As mentioned earlier, Erickson and Brandon [16] and Hall [17] have shown that the wing-vortex breakdown could be delayed through the interaction of the chined-forebody vortex. Therefore, the asymmetric breakdown of the chined-forebody vortex would cause a differential interaction to

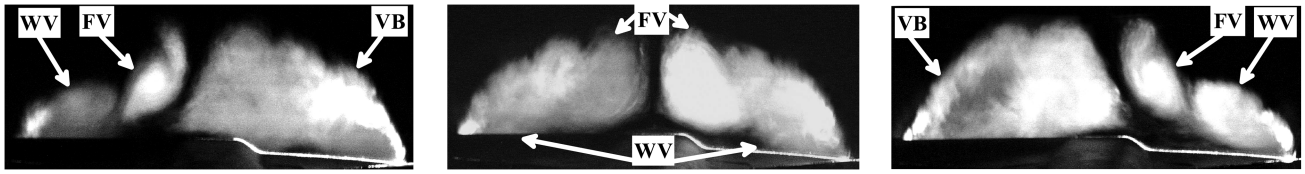

a) Left disturbance b) No disturbance c) Right disturbance

Fig. 10 Smoke-flow visualization photographs for wing–body (without strake), at section S13, $\alpha = 34.5$ deg, $Re = 0.15 \times 10^6$.

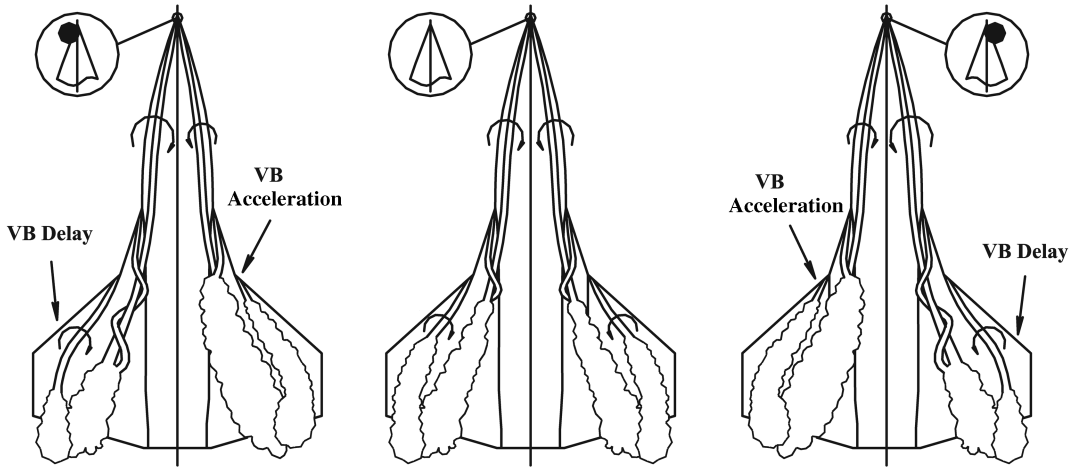

a) Left disturbance b) No disturbance c) Right disturbance

Fig. 11 Schematic diagram of disturbance effects on asymmetric vortex breakdown.

the vortices on the left and right side of the wing. Specifically, the delay of the wing-vortex breakdown became weaker on the side of the acceleration of the forebody-vortex breakdown and became stronger on the other side. Consequently, the wing-vortex breakdown also became asymmetric.

In addition, it should be noted that the chined-forebody vortex also interacted with the strake vortex besides the wing vortex. However, the strake vortex did not influence the response of the chined-forebody vortex to the tip disturbance, as shown in Fig. 10. It only twisted together with the chined-forebody vortex and enhanced the intensity of the forebody vortex [18]. Therefore, the main conclusions of the experiments would be the same with or without the strake.

B. Control of Asymmetric Vortex Breakdown

The methods for flight control by the manipulation of the vortex flow around aircraft at high angles of attack have been paid more attention in recent years [3,4,10–13,19–21], because the separated flow is dominant at high angles of attack, whereas the traditional control methods, such as elevator, rudder, and aileron, are inefficient and even ineffective at this time. The controllable vortex available focused on the forebody vortex and the leading-edge vortex of a wing. Recently, Huang et al. [19] implemented the flight control of a model aircraft with a delta-wing configuration for all three axes by distributing microelectromechanical system (MEMS) devices along the round leading edge to control the leading-edge vortex. For the research on the control of the smoothed-side forebody-vortex, the results were too many [3,4], because the asymmetric vortex would be produced over it and could provide enough yaw control moments. The recent studies [20] about it have extended the control scheme from open-loop to closed-loop control to obtain a more robust control system. In addition, some researchers [21,22] also found that the vortex over the smoothed-side forebody could influence the wing loads and induce roll moments, and so could implement the control for yaw and roll together.

However, the vortex flow over the chined forebody is very different from the one over the smoothed forebody, and it has no asymmetry like the smoothed-forebody vortex and is more readily broken down. The control of vortex breakdown was a very important issue and was studied extensively in the flow control field [23], but the research to control vortex breakdown by a tip disturbance was quite little, especially for the control of asymmetric vortex breakdown. Lowson and Riley [14] conducted an experimental study on the control of vortex breakdown over delta wings by using an apex flap (it could make vortex-breakdown points delay or move forward), but the asymmetric control was not considered. The present experimental results about the chined forebody demonstrate that the level of the asymmetric vortex breakdown could vary with the geometric sizes of the tip disturbance, as shown in Fig. 8. This implies that the asymmetric vortex breakdown could be controlled proportionally by using a variable tip disturbance. The asymmetric vortex breakdown could induce a large asymmetric load on the wing, and so this seems to hold a promise of the aircraft's rolling control at high angles of attack. However, the controllability for roll needs to be verified further, such as by free-to-roll experiments.

V. Conclusions

1) The vortices of a chined forebody could produce asymmetric breakdown by adding an artificial disturbance onto the nose tip at high angles of attack. The forebody vortex with asymmetric breakdown would further interact with the vortices over the strake and wing, and also cause them to produce asymmetric breakdown. As a result, the significantly asymmetric pressure distribution was induced on the two sides of the wing.

2) The magnitude and positions of the artificial tip disturbance could influence the level of the asymmetric vortex breakdown. The asymmetry level increased with the increase of the geometric sizes of the tip disturbance. This seems to hold a promise to control proportionally the asymmetric vortex breakdown by using a variable tip disturbance. Moreover, the disturbance has a more prominent effect on the asymmetric breakdown when the tip disturbance is located on the leeward side and approaches the nose tip.

3) The asymmetry of vortex breakdown would disappear when a splitter plate was placed in the leeward symmetry plane of the model

even by adding a tip disturbance. This implies that the interaction of the forebody vortex itself would play a key role on the asymmetric vortex breakdown.

Acknowledgments

The project is supported by the National Natural Science Foundation of China (10432020 and 10702004) and China Postdoctoral Science Foundation (20060390397).

References

[1] Hunt, B. L., "Asymmetric Vortex Forces and Wakes on Slender Bodies," AIAA Paper 82-1336, Aug. 1982.

[2] Deng, X. Y., Wang, G., Chen, X. R., Wang, Y. K., Liu, P. Q., and Xi, Z. X., "Physical Model of Asymmetric Vortices Flow Structure in Regular State over Slender Body at High Angle of Attack," *Science in China Series E*, Vol. 46, No. 6, 2003, pp. 561–573. doi:10.1360/02ye0164

[3] Willims, D. R., "Review of Forebody Vortex Control Scenarios," AIAA Paper 97-1967, June 1997.

[4] Roos, F. W., "Microblowing: an Effective, Efficient Method of Vortex Asymmetry Management," AIAA Paper 2000-4416, Aug. 2000.

[5] Roos, F. W., and Kegelman, J. T., "Aerodynamic Characteristics of Three Generic Forebody at High Angles of Attack," AIAA Paper 91-0275, Jan. 1991.

[6] Kegelman, J. T., and Roos, F. W., "Influence of Forebody Cross-Section Shape on Vortex Flowfield Structure at High Alpha," AIAA Paper 91-3250, Sept. 1991.

[7] Mange, R. L., and Roos, F. W., "Aerodynamics of a Chined Forebody," AIAA Paper 98-2903, June 1998.

[8] Lowson, M. V., and Ponton, A. J. C., "Symmetry Breaking in Vortex Flows on Conical Bodies," *AIAA Journal*, Vol. 30, No. 6, 1992, pp. 1576–1583.

[9] Stahl, W. H., Mahmood, M., and Asghar, A., "Experimental Investigations of the Vortex Flow on Delta Wings at High Incidence," *AIAA Journal*, Vol. 30, No. 4, 1992, pp. 1027–1032.

[10] Williams, S. P., and Garry, K. P., "Experimental Investigation into Yaw Control at Alpha on a Chined Forebody Using Slot Blowing," *The Aeronautical Journal*, Vol. 100, No. 998, Oct. 1996, pp. 355–363.

[11] Arena, A. S., Jr., Nelson, R. C., and Schiff, L. B., "Directional Control at High Angles of Attack Using Blowing Through a Chined Forebody," *Journal of Aircraft*, Vol. 32, No. 3, 1995, pp. 596–602.

[12] Cummings, R. M., Schiff, L. B., and Duino, J. D., "Experimental Investigation of Tangential Slot Blowing on Generic Chined Forebody," *Journal of Aircraft*, Vol. 32, No. 4, 1995, pp. 818–824.

[13] O'Rourke, M., "Experimental Investigation of Slot Blowing for Yaw Control on a Generic Fighter Configuration with a Chined Forebody," AIAA Paper 95-1798, June 1995.

[14] Lowson, M. V., and Riley, A. J., "Vortex Breakdown Control by Delta Wing Geometry," *Journal of Aircraft*, Vol. 32, No. 4, 1995, pp. 832–838.

[15] Chen, X. R., Deng, X. Y., Wang, Y. K., Liu, P. Q., and Gu, Z. F., "Influence of Nose Perturbations on Behaviors of Asymmetric Vortices over Slender Body," *Acta Mechanica Sinica*, Vol. 18, No. 6, 2002, pp. 581–593. doi:10.1007/BF02487960

[16] Erickson, G. E., and Brandon, J. M., "On the Nonlinear Aerodynamic and Stability Characteristics of a Generic Chine-Forebody Slender-Wing Fighter Configuration," NASA 89447, June 1987.

[17] Hall, R., "Influence of Forebody Cross-Sectional Shape on Wing Vortex-Burst Location," *Journal of Aircraft*, Vol. 24, No. 9, 1987, pp. 645–652. doi:10.2514/3.45490

[18] Ma, B. F., and Deng, X. Y., "Vortex Interactions Between Chined-Forebody and Strake," *Journal of Aircraft*, Vol. 43, No. 6, 2006, pp. 1953–1956. doi:10.2514/1.25898

[19] Huang, A., Folk, C., Silva, C., Christensen, Y., Chen, Y., Ho, C. M., Jiang, F., Grosjean, C., Tai, Y. C., Lee, G. B., Chen, M., and Newbern, S., "Application of MEMS Devices to Delta Wing Aircraft: From Concept Development to Transonic Flight Test," AIAA Paper 2001-0124, June 2001.

[20] Patel, M. P., Tilmann, G. P., and Ng, T. T., "Closed-Loop Missile Yaw Control via Manipulation of Forebody Flow Asymmetries," *Journal of Spacecraft and Rockets*, Vol. 41, No. 3, 2004, pp. 436–443. doi:10.2514/1.10701

[21] Peterson, K. G., Darden, L. A., and Komerath, N. M., "Dynamic Roll Control Experiments Using a Movable Nosetip," AIAA Paper 96-0789, June 1996.

[22] Nelson, P., "Experiments in Aircraft Roll-Yaw Control Using Forebody Tangential Blowing," Ph.D. Dissertation, Dept. of Aeronautics and Astronautics, Stanford Univ., Palo Alto, CA, 1997.

[23] Mitchell, A. M., and Delery, J., "Research into Vortex Breakdown Control," *Progress in Aerospace Sciences*, Vol. 37, No. 4, 2001, pp. 385–418. doi:10.1016/S0376-0421(01)00010-0